Velocity Distributions in Taylor Vortex Flow with Imposed Laminar Axial Flow and Isothermal Surface Heat Transfer

D. A. Simmers† and J. E. R. Coney‡

Fully-developed flow in a concentric annulus formed by a stationary outer cylinder, which may be heated isothermally, and a rotatable inner cylinder has been studied experimentally by means of hot-wire anemometry techniques. Velocity profiles for the axial, tangential, and radial directions of flow have been obtained for adiabatic and diabatic conditions and for wide and narrow annular gaps.

It has been shown that the onset of Taylor vortex flow has a pronounced effect on the velocity profiles for all three directions. However, while the profiles for the axial and tangential directions are explicable, those for the radial direction are not so, at present. Also, it was found that heat transfer through the outer annular surface had a greater effect on the radial velocity profile than on the axial or tangential, but in the narrow gap case only.

NOTATION

b annular gap width $(R_2 - R_1)$
d_e equivalent diameter of annulus $\{2(R_2 - R_1)\}$
N annular radius ratio (R_1/R_2)
R general radial co-ordinate
R_1 radius of inner annular surface
R_2 radius of outer annular surface
R' dimensionless radial gap position $(R_2 - R)/(R_2 - R_1)$
Re_a axial Reynolds number $\{(u_a)_{av} d_e/\nu\}$
Ta Taylor number, $(2\Omega_1^2 R_1^2 b^3)/\{\nu^2(R_1 + R_2)\}$ (wide gap case)
u velocity component
ν kinematic viscosity of fluid
Ω_1 angular velocity of inner annular surface

Subscripts

a axial flow direction
av average value
r radial flow direction
t tangential flow direction

INTRODUCTION

In reference (1), the authors presented a method for determining the velocity distributions in the axial, tangential, and radial directions, prevailing in an annulus, the outer surface of which was stationary while the inner surface was rotatable. Using hot-wire anemometry methods, they showed that it was possible to separate the three velocity components from two readings taken from a single probe. Also, in reference (1), they gave typical examples of velocity profiles obtained by this method.

However, their experimental investigation extended beyond the conditions of the few examples given in reference (1), taking into account, for fully developed flow, two annular radius ratios, several imposed axial flows, and the effect of isothermally heating the outer surface of the annular gap. A number of the profiles obtained are given in the present work, showing both the marked effect of Taylor vortex flow and that of the isothermal heating of the annular outer surface.

† UKAEA, Risley, Warrington, WA3 6AT, UK
‡ Department of Mechanical Engineering, University of Leeds, Leeds, LS2 9JT, UK
Received 1 October 1979 and accepted for publication on 8 February 1980.

2 EXPERIMENTAL TECHNIQUES AND APPARATUS

The experimental techniques and apparatus employed are described in reference (1). However, in reference (1) only tests made under adiabatic conditions are described whereas, in the present investigation, both adiabatic and diabatic conditions are considered. For the latter case, the outer stationary surface of the annular gap was heated by passing wet steam through the annular jacket surrounding it. Since the heating medium was wet steam, and the working fluid in the annular gap was air, it was possible to maintain the outer stationary surface isothermal. A surface temperature of 100°C was used throughout the investigation, being determined by nine chromel-alumel thermocouples arranged in three equal and equispaced groups at each end and at the middle of the annular gap.

The air was admitted from the laboratory and preheated so that its temperature at inlet was approximately 65°C, rising to a mean temperature in the range of 85°C to 90°C at the section where results were taken. The inner cylinder was of Tufnol and hence formed an adiabatic boundary.

Throughout the tests, care was taken to ensure that measurements were made in the region of fully-developed flow. The development of annular flow had been studied earlier by the authors and their findings are described in reference (2).

3 PRESENTATION AND DISCUSSION OF RESULTS

3.1 Axial Velocity Distribution

Axial velocity profiles are presented in Fig. 1 for $N = 0{\cdot}955$ and $Re_a = 1200$ and for both adiabatic and diabatic flows. It may be seen that the effect of an imposed temperature gradient at the outer annular surface has little effect when the inner annular surface is

0142/727X/80/0600-0085$02.00

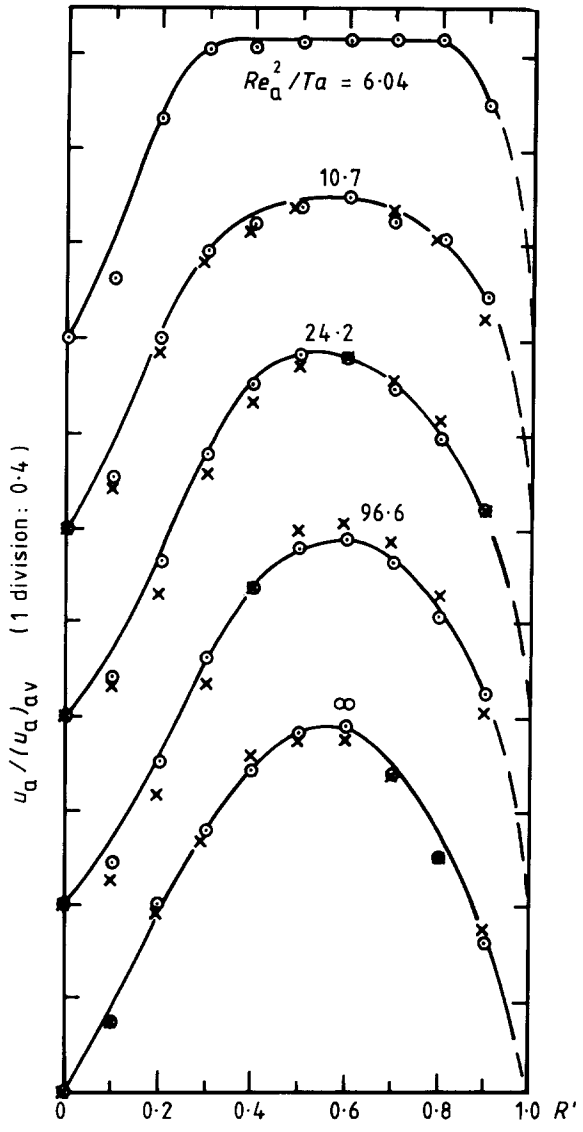

Fig. 1. Axial velocity profiles. $N = 0{\cdot}955$, $Re_a = 1200$. ⊙—⊙ Adiabatic conditions; ×—× Diabatic conditions

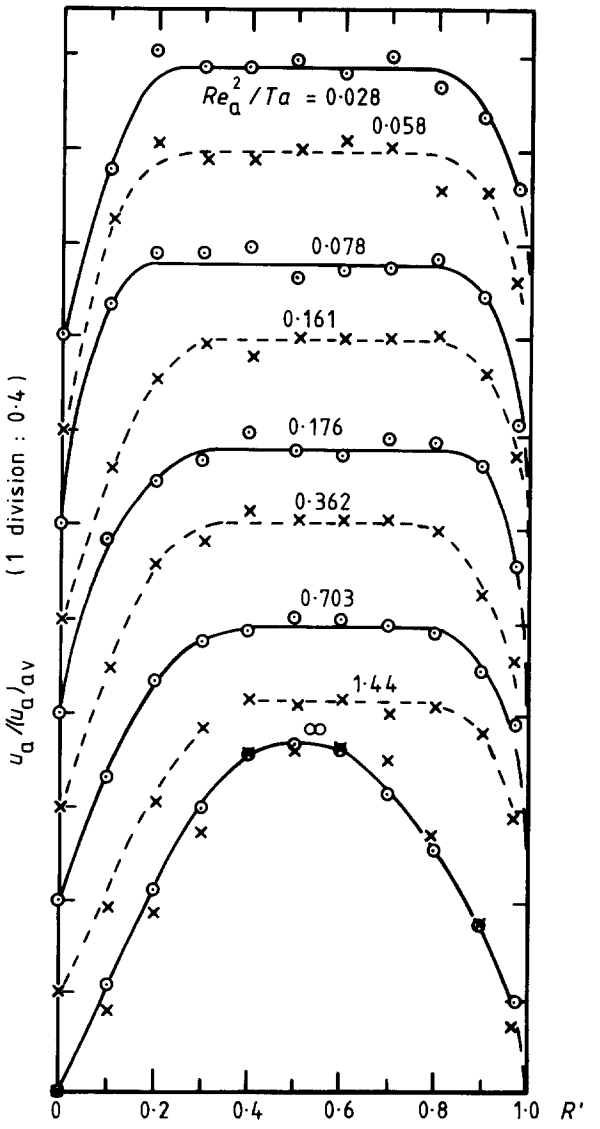

Fig. 2. Axial velocity profiles. $N = 0{\cdot}8$, $Re_a = 400$. ⊙—⊙ Adiabatic conditions; × – – × Diabatic conditions

stationary. Also, at $Re_a^2/Ta = 96{\cdot}6$, Couette flow still prevailing, $u_a/(u_a)_{av}$ for diabatic flow is similar at a given value of R' to that for adiabatic flow. At and after criticality ($Re_a^2/Ta \leq 24{\cdot}2$) there is still little difference between adiabatic and diabatic conditions.

As was pointed out in reference (**1**), after the onset of Taylor vortex flow, the profile becomes increasingly flattened as Re_a^2/Ta decreases. This effect is now seen to exist for both adiabatic and diabatic flows.

Results for $N = 0{\cdot}955$ and $Re_a = 400$ will not be presented here since they appear in reference (**1**). However, comparison of these results with those of Fig. 1 shows little variation which may be imputed to the difference in axial Reynolds number.

The results for an annular radius ratio of 0·8 are shown in Figs. 2 and 3. (The adiabatic flow results of Fig. 3 also appear in Fig. 3(c) of reference (**2**), where they were used merely to show the limits of developing flow, which that paper considers.) These results cover a much higher Taylor number range and the flattened 'core' region is seen to widen with decreasing Re_a^2/Ta, eventually occupying about 65 per cent of the total gap width at the highest value of Taylor number investigated, and moving axially at $u_a/(u_a)_{av} = 1{\cdot}15$. All of the results presented in Figs. 2 and 3 indicate that an inward skew of the axial velocity profile occurs in the vortex regime, in which very high velocity gradients occur close to the walls, although the observed gradients close to the inner wall may be higher than those actually obtaining, as was discussed in (**1**).

Assuming that the flattened 'core' of the profile indicates that the vortices move axially as a body, it may be seen from Fig. 1 that, in the Taylor number range investigated for $N = 0{\cdot}955$, the vortices occupy up to 50 per cent of the gap width, whereas at the higher Taylor numbers of $N = 0{\cdot}8$ (Figs. 2 and 3), they occupy up to 65 per cent of the gap. Although this suggests that the more energetic vortices, associated with high Taylor numbers, occupy more of the gap width, there is some evidence to suggest that this is not the case. Oscilloscope traces (Fig. 4) for $N = 0{\cdot}955$, $Re_a = 400$ (the conditions of Fig. 6 in (**1**)) and $Re_a^2/Ta = 6{\cdot}01$ indicate that the vortices occupy a larger proportion of the gap than suggested by the flattened region of the axial velocity profiles. Referring to Fig. 6 in reference (**1**), the flattened region is seen to occupy a maximum of 40 per cent of the gap width,

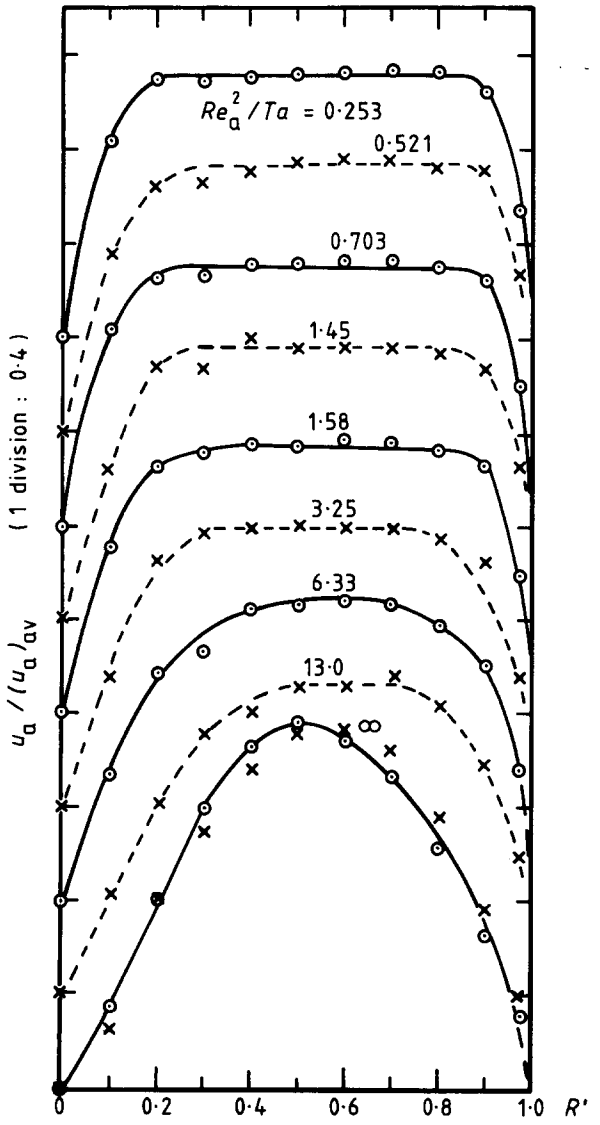

Fig. 3. Axial velocity profiles. $N = 0{\cdot}8$, $Re_a = 1200$. ⊙—⊙ Adiabatic conditions; × -- × Diabatic conditions

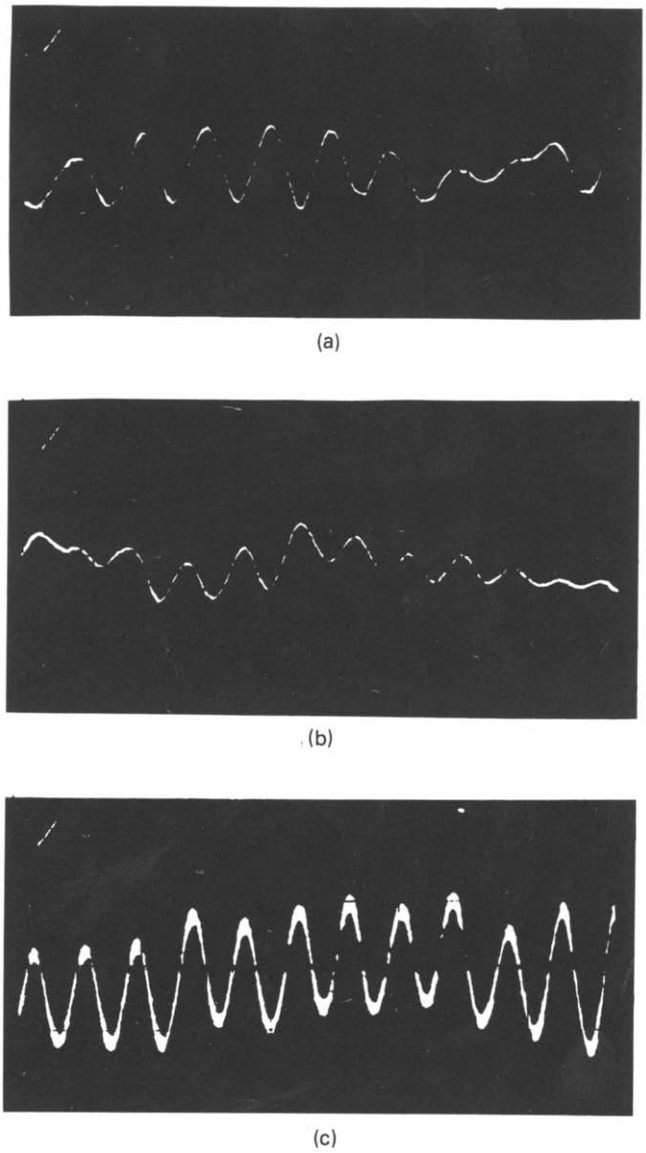

Fig. 4. Hot-wire probe outputs at various radial positions, $Re_a = 400$, $Re_a^2/Ta = 6{\cdot}01$, $N = 0{\cdot}955$, sensitivity = 5 mV/div. (a) $R' = 0{\cdot}1$; (b) $R' = 0{\cdot}5$; (c) $R' = 0{\cdot}9$

whereas the vortices are apparent in all of the oscilloscope traces, taken at three positions covering 80 per cent of the gap width. Thus the flattened region does not correspond to the radial extent of the vortices, and although the central portion of the vortex cell can move as a solid body, the outer regions must be subjected to considerable shear.

Professor K. N. Astill reported to the authors that in a flow visualization apparatus of radius ratio 0·57, with air as the working fluid and smoke as the flow visualization medium, he had observed that the vortices, when viewed from the outer surface, appeared to pass through the smoke-filled air. Although the axial velocity of the fluid close to the outer wall was indicated by the drifting smoke, the vortices were observed to be moving faster than the drifting fluid. This, in conjunction with the results presented here, suggests that the vortices move bodily in the axial direction. However, the outer portions of the vortex cells must pass through the fluid rather than move with it, resulting in the shear indicated by the present results. Although the vortices probably occupy the same proportion of the gap for both $N = 0{\cdot}955$ and 0·8, in the case of $N = 0{\cdot}8$, the higher Taylor numbers investigated result in more energetic vortices, which are capable of dragging more fluid along at the vortex drift velocity. Thus, a more flattened velocity profile occurs, as indicated by the results.

In reference (3), results are reported of an investigation made into this problem, by correlation techniques, for $N = 0{\cdot}8$ and 0·955, but with the flow just critical. The axial wave drift velocity ratios at criticality were found for $Re_a \leqslant 1200$ and these values differ from the values of $u_a/(u_a)_{av}$ presented in Figs. 1–3. It is suggested that the differences between these results and those of the present investigation offers qualitative support for the mechanism discussed above.

The mass rate of flow of the air through the annular gap was determined using orifice plates, designed according to British Standards Specification 1024 and checked by velocity measurements within the gap, using a hot-wire wire probe. For $Ta = 0$ and $Re_a < 2500$, there was an average discrepancy of some 3 per cent between the two values. For $Ta > 0$, experimental values of $(u_a)_{av}$ were compared with a theoretical value estimated

from $Re_a = 400$, $N = 0{\cdot}955$ and a mean fluid temperature of 25°C. It was found that, as Re_a^2/Ta increased from 0·671 to 10·7, so the ratio of the experimental to the theoretical value of $(u_a)_{av}$ fell from 1·23 to 0·91. A fuller treatment of this matter appears in reference (1).

3.2 Tangential Velocity Distribution

Figures 5–7 show tangential velocity profiles for $N = 0{\cdot}955$, $Re_a = 400$ and 1200 and for $N = 0{\cdot}8$, $Re_a = 400$. Those for $N = 0{\cdot}8$, $Re_a = 1200$, were omitted since they added little to the data of Fig. 7. In these carpet plots, the tangential velocity is normalized with respect to the velocity of the inner surface of the annular gap.

The results for $N = 0{\cdot}955$ show the effects of the transition from the straight line distribution of Couette flow to that for Taylor vortex flow (Figs. 5 and 6). As was pointed out in reference (1), the distribution for Taylor vortex flow is shown to be characterized by a central region of relatively small velocity gradient, bounded by regions of high velocity gradients close to the annular boundaries, the highest gradient occurring near the inner surface. The gradient across the central region seems to be dependent on the value of Re_a^2/Ta, a

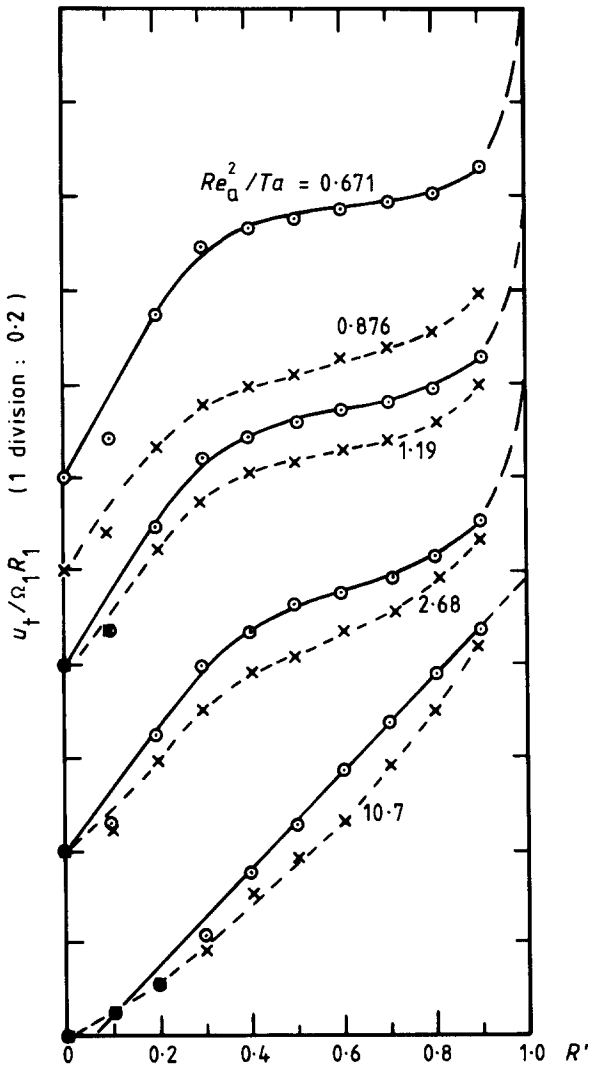

Fig. 5. Tangential velocity profiles. $N = 0{\cdot}955$, $Re_a = 400$. ⊙—⊙ Adiabatic conditions; × -- × Diabatic conditions

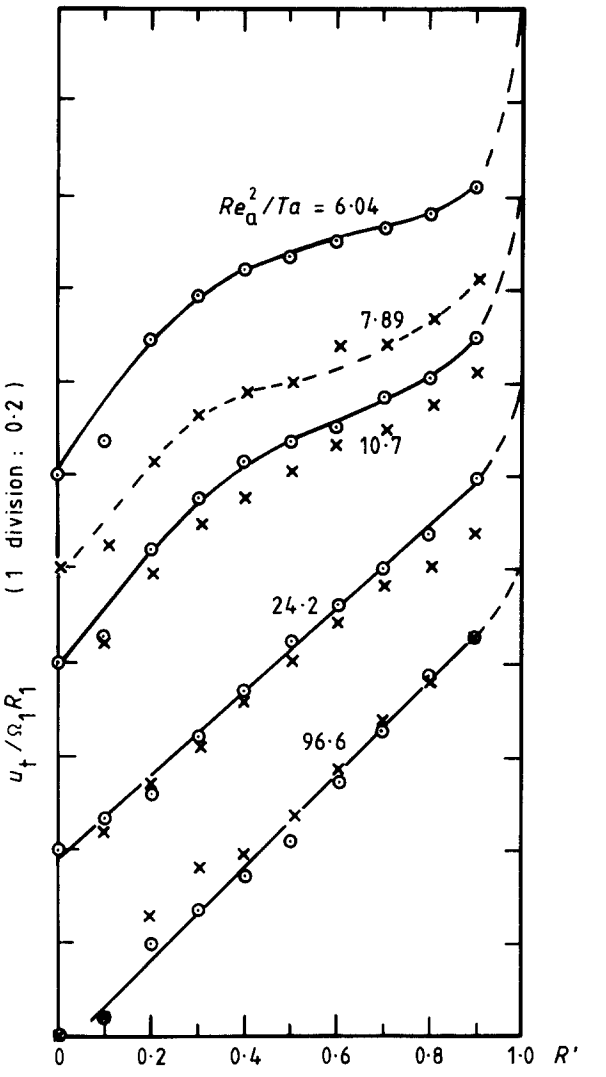

Fig. 6. Tangential velocity profiles. $N = 0{\cdot}955$, $Re_a = 1200$. ⊙—⊙ Adiabatic conditions; × -- × Diabatic conditions

decrease in slope resulting from a decrease in Re_a^2/Ta. As for the axial velocity profiles, this central region occupies up to 50 per cent of the gap width and is characterized by a velocity change of $u_t/\Omega_1 R_1 = 0{\cdot}4$ to 0·6 at low Taylor numbers, and by $u_t/\Omega_1 R_1 = 0{\cdot}4$ to 0·5 at higher Taylor numbers.

In addition, comparison of Figs. 5 and 6 shows that criticality does not occur at a constant value of Re_a^2/Ta, since under differing values of axial flow the profiles are markedly different. For $Re_a = 400$ and $Re_a^2/Ta = 10{\cdot}7$ (Fig. 5), the distribution exhibits the straight line relationship of Couette flow; at $Re_a = 1200$ and $Re_a^2/Ta = 10{\cdot}7$ (Fig. 6), the presence of vortices is indicated by the flattened central portion of the velocity distribution.

For $N = 0{\cdot}8$ (Fig. 7), all the profiles indicate the presence of supercritical flow. The flattened central region occupies up to 70 per cent of the gap width, but the slope of this region seems to be much less dependent on Re_a^2/Ta and the velocity change remains virtually constant at $u_t/\Omega_1 R_1 = 0{\cdot}3$ to 0·4.

Considerations regarding the flattening of the tangential profile, are the same as those in Section 3.1 related to the axial velocity profile. Thus, it is suggested that, in the tangential direction, the vortices rotate as solid bodies, while their outer edges actually move through, rather

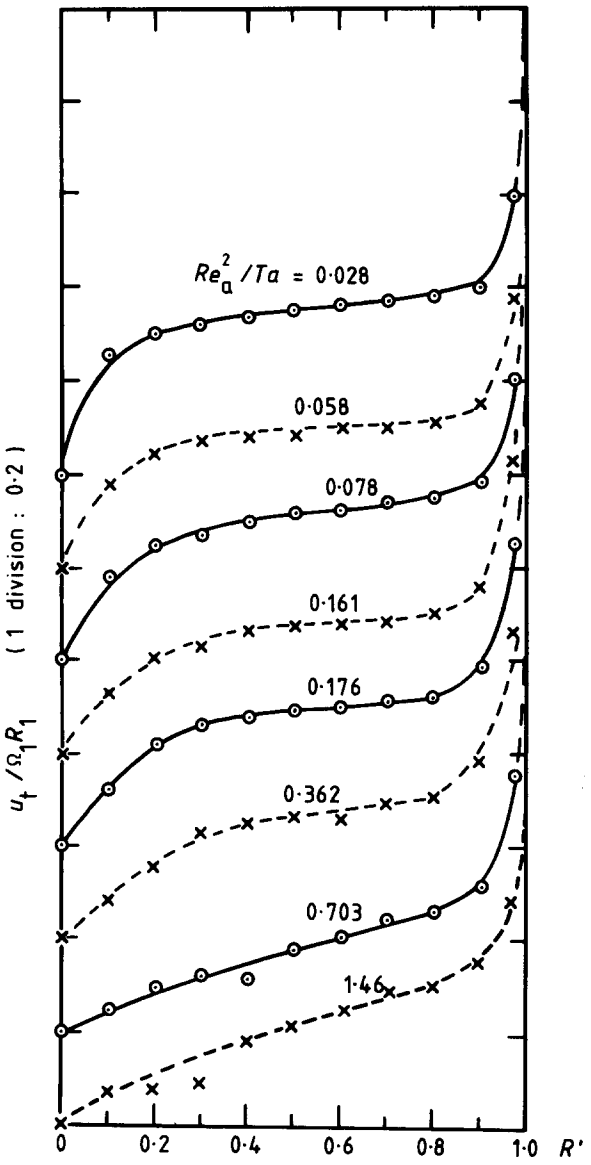

Fig. 7. Tangential velocity profiles. $N = 0{\cdot}8$, $Re_a = 400$. ⊙—⊙ Adiabatic conditions; × -- × Diabatic conditions

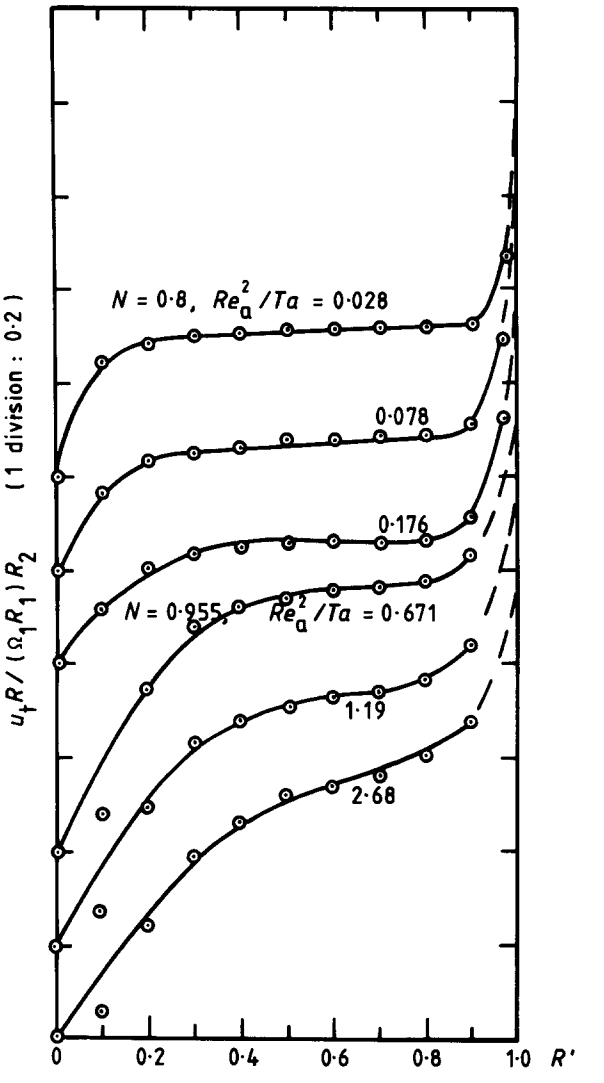

Fig. 8. Adiabatic tangential velocity profiles for $Re_a = 400$, replotted in terms of $u_t R/(\Omega_1 R_1)R_2$

than with, the fluid. Again, at the lower range of Taylor numbers investigated for $N = 0{\cdot}955$, the vortices have insufficient energy to drag much fluid around at the tangential velocity of the vortices, resulting in the larger velocity gradients encountered at this radius ratio. At the higher Taylor number range investigated for $N = 0{\cdot}8$, the central region is much flatter because of the effects of the more energetic vortices, which induce more fluid to rotate at the tangential velocity of the vortices.

The velocity distribution typical of the present study is more in accord with that found by Taylor (4) in that a small velocity gradient was observed across the central region of the gap, in contradiction to the findings of Pai (5), which suggested that a constant mean velocity, equal to half the velocity of the inner annular surface, existed across 60 per cent of the gap. Accordingly, data from Figs. 5 and 7 were replotted in terms of $u_t R/(\Omega_1 R_1)R_2$ to check for constancy of $u_t R$, as found by Taylor (4), and are presented in Fig. 8. The results suggest that, in the lower Taylor number range investigated for $N = 0{\cdot}955$, no such constancy exists; however, in the higher range, for $N = 0{\cdot}8$, a constant value of $u_t R$ exists over about 70 per cent of the gap width. The results of Taylor (4) were obtained at a very high value of Taylor number ($Ta = 1{\cdot}056 \times 10^{10}$), and the present results confirm those results for such high Taylor numbers.

In reference (3), it is demonstrated that, at criticality, the vortices occupy the whole of the annular gap if $Re_a \leqslant 160$. As Re_a increases, so the vortex width decreases until, for $800 \leqslant Re_a \leqslant 1200$, the vortex occupies 40 per cent of the gap width, adjacent to the inner cylinder, for $N = 0{\cdot}955$ and 50 per cent for $N = 0{\cdot}8$. These findings support the results of Figs. 5–7, which show that, after criticality, the vortex is closer to the inner cylinder than to the outer. However, the correspondence in vortex width between the two investigations is closer for $N = 0{\cdot}955$ than for 0·8.

Turning now to the effect of isothermally heating the stationary outer surface of the annular gap, adiabatic and diabatic results for $N = 0{\cdot}955$ (Figs. 5 and 6) were taken under identical conditions of Re_a^2/Ta. Figure 5 indicates that the adiabatic and diabatic profiles are similar for $Re_a = 400$ and $Re_a^2/Ta = 10{\cdot}7$, 2·68, and 1·19, differing in terms of $u_t/\Omega_a R_1$ by no more than 10 per cent.

This suggests the vortices are in the same state under both adiabatic and diabatic conditions, indicating that

the radial temperature difference of the present study, which was within the limits of 15°C to 30°C, has no significant effect on the critical Taylor number.

This observation is in accordance with that of Sorour and Coney (**6**) who found that, in an annular gap of $N = 0{\cdot}955$, there was no difference in the critical Taylor number as between adiabatic and diabatic flows for $Re_a < 1300$.

The adiabatic and diabatic results for $N = 0{\cdot}8$ were taken at identical speeds of rotation of the inner annular surface, namely, 200, 400, 600, and 1000 rev/min and are presented in Fig. 7. For a given rotational speed, the Taylor number for adiabatic flow is always higher than that for diabatic flow, because of the dependence of the Taylor number on the kinematic viscosity and thus on the temperature of the working fluid. Hence, these results illustrate the importance of the working temperature in such a system. Considering convective heat transfer at the outer stationary annular surface, a considerable drop of Nusselt number could result if the working temperature is increased while the operating speed remains constant, owing to the reduction of the Taylor number. In the worst case, the flow could pass from supercritical to the subcritical regime, resulting in a markedly reduced heat transfer performance.

Also in Fig. 7, the results for $Re_a^2/Ta = 0{\cdot}176$ (adiabatic) and $Re_a^2/Ta = 0{\cdot}161$ (diabatic) again show the similarity of adiabatic and diabatic profiles for similar values of Re_a^2/Ta, and with a constant value of axial Reynolds number. Sorour and Coney (**6**) also found that for $N = 0{\cdot}8$, and the values of Re_a under consideration, there was only a small difference between critical Taylor numbers for adiabatic and diabatic flow, with the air flowing downward through the annular gap, as in the present tests.

3.3 Radial Velocity Distributions

Figures 9 and 10 present the radial velocity distributions for $N = 0{\cdot}955$ and $0{\cdot}8$, for $Re_a = 400$ and 1200, and for both adiabatic and diabatic flow conditions. Unlike the axial and tangential velocities, the radial component has not been normalized since there is no reference velocity for this purpose. The profiles give the distribution of the r.m.s. amplitude of the fluctuating radial component and not that of the mean velocity component.

In all of the tests, the radial velocity was found to be the least significant velocity component and, in many cases, was an order of magnitude smaller than the axial and tangential velocity components. Consequently, the results for this case are likely to be subjected to far greater errors than previously encountered.

Of the three velocity components under consideration, the present results are the most interesting and least explicable. Under all of the above conditions, the velocity profiles are characterized by dual peaks at $R' \approx 0{\cdot}2$ and $0{\cdot}9$, these having no reflection in the corresponding axial and tangential velocity profiles. Also, greater differences occur between adiabatic and diabatic flow profiles than for axial and tangential flows. For example, in Fig. 5, the adiabatic and diabatic tangential velocity profiles for $Re_a^2/Ta = 2{\cdot}68$ are little different. However, in Fig. 9(a), a considerable difference occurs at this value. In the adiabatic case, the profile is flattened and is of the form which might be expected near to criticality. For diabatic flow, the velocities are much greater; there is a maximum value near to the outer stationary cylinder

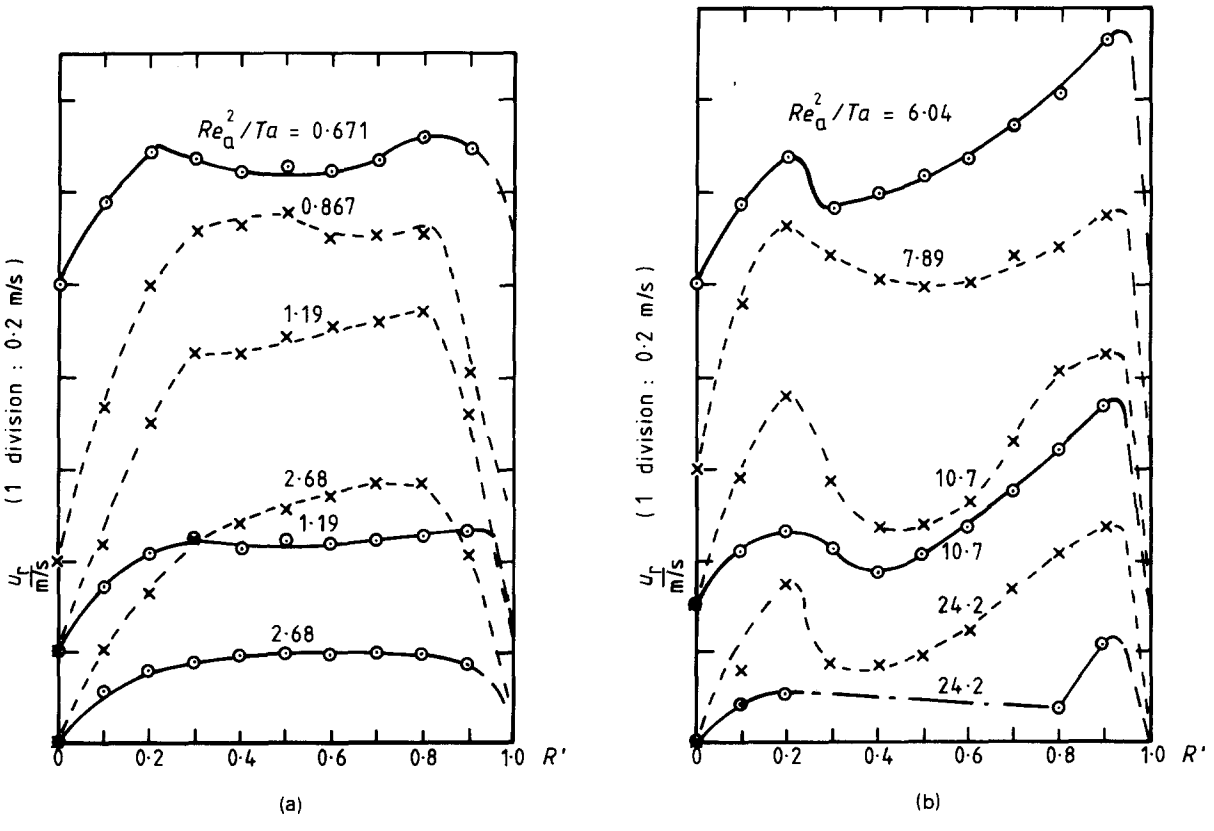

Fig. 9. Radial velocity profiles. $N = 0{\cdot}955$. (a) $Re_a = 400$; (b) $Re_a = 1200$. ⊙—⊙ Adiabatic conditions; × -- × Diabatic conditions

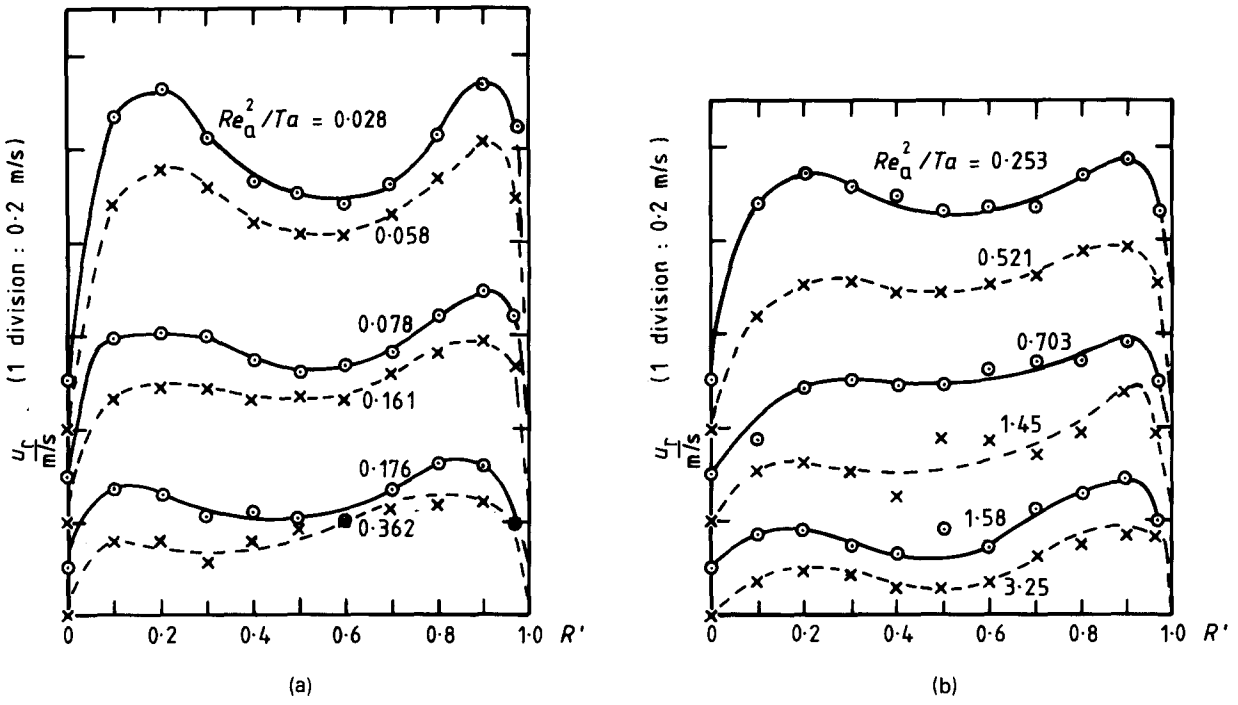

Fig. 10. Radial velocity profiles. $N = 0{\cdot}8$. (a) $Re_a = 400$; (b) $Re_a = 1200$. ⊙—⊙ Adiabatic conditions; × -- × Diabatic conditions

and the beginning of the dual-peak distribution may be discerned. Also, as Re_a^2/Ta decreases, so the difference between the adiabatic and diabatic flow profiles is accentuated. Considering now the results for $Re_a = 1200$ in Fig. 9(b) and comparing them with those having the same value of Re_a^2/Ta in Figs. 1 and 6, it appears from the latter figures that, at $Re_a^2/Ta = 24{\cdot}2$, there is little evidence of Taylor vortices. In Fig. 9(b), however, both the adiabatic and diabatic velocity profiles show the dual-peak form. Again, as for $Re_a = 400$, the velocities for the diabatic case are markedly higher than those for the diabatic.

The results for $N = 0{\cdot}8$ (Fig. 10) contradict to some extent those of Fig. 9. Although the dual-peak form is evident and although diabatic conditions give higher velocities than adiabatic, the former effect is much more evident at $Re_a = 400$ than $Re_a = 1200$.

As was stated in reference (1), a physical explanation cannot be offered for these radial velocity profiles, especially as they have little correspondence with their axial and tangential counterparts. It is doubtful if the dual peaks correspond to the limits of the flattened region of the axial profiles or to the central region of small gradient of the tangential profiles; these two latter regions extend with decrease in Re_a^2/Ta, whereas the dual peaks maintain a constant separation. All that can be said is that the radial velocities are much more affected by heat transfer through the outer stationary surface than are the axial or tangential velocities and that the radial position of the dual peaks is invariant. However, this latter constancy may be taken as an indication that, once the vortices have appeared, their form remains unchanged within the limits of the present investigation.

4 CONCLUSIONS

Velocity data for a fully-developed, three-dimensional velocity field induced by the presence of Taylor vortex flow, having a superimposed axial flow, have been presented for two values of radius ratio, $N = 0{\cdot}8$ and $0{\cdot}955$, for various values of Taylor number with axial Reynolds numbers of $Re_a = 400$ and 1200; these data were representative of the results found for the axial Reynolds number range of $300 \leqslant Re_a \leqslant 1600$. The effects of Taylor vortices on the axial and tangential velocity components were noted, and physical mechanisms for these effects were suggested, indicating that certain portions of the vortices move through, rather than with, the working fluid. The physical meaning of the observed radial velocity profile, however, could not be adequately explained.

The parameter Re_a^2/Ta was found to be unimportant in describing the relationship between the axial Reynolds number and the critical Taylor number for initial vortex onset. However, this parameter was shown to be useful as a similarity parameter for the tangential profiles obtained for a constant value of axial Reynolds number but with varying fluid temperatures, suggesting that the radial temperature differences encountered in the present study had no significant effect on criticality.

REFERENCES

(1) SIMMERS, D. A. and CONEY, J. E. R. 'The experimental determination of velocity distribution in annular flow', *Int. J. Heat & Fluid Flow* 1979, **1** (no. 4), 177–184

(2) SIMMERS, D. A. and CONEY, J. E. R. 'The effect of Taylor vortex flow on the development length in concentric annuli', *J. Mech. Engng. Sci.* 1979, **21**, (No. 2), 59–64

(3) SOROUR, M. M. and CONEY, J. E. R. 'An experimental investigation of the stability of spiral vortex flow', *J. Mech. Engng. Sci.* 1979, **21**, 397–402

(4) TAYLOR, G. I. 'Distribution of velocity and temperature between concentric rotating cylinders', *Proc. Roy. Soc. (Lond.) Series A* 1935, **151**, 494–512

(5) PAI, S. I. 'Turbulent flow between rotating cylinders', 1943 NACA Tech Note No. 892

(6) SOROUR, M. M. and CONEY, J. E. R. 'The effect of temperature gradient on the stability of flow between vertical concentric rotating cylinders', *J. Mech. Engng. Sci.* 1979, **21**, 403–409